Title

An Assessment of Aerial Firefighting Response Times Between Agencies During the 2020 Fire Season in California

Abstract

Rapid, well-coordinated aerial response can be an effective way to limit wildfire growth during the initial-response (IR) period. To date, most quantitative studies of wildland fire aviation effectiveness have relied on data from aircraft provided by the United States Forest Service (USFS), while other agencies aircraft have received less attention. This study leverages open ADS-B data to reconstruct second-by-second aircraft movements for both the CAL FIRE and USFS aircraft during the 2020 California fire season, allowing a comparison between use of different agency aircraft for the first time. This study characterizes the two fleets activity and identifies how landscape, weather, and values-at-risk influence time to first aircraft arrival within the first 24 hours after ignition. ADS-B flight tracks for USFS and CAL FIRE aircraft were matched to 7,214 wildfires; response time was calculated as the interval between ignition discovery and the first ADS-B detection within 5 km. Cause-specific cumulative-incidence curves compared the probability that each agency arrived first, while Cox proportional-hazards models, with stratification by diurnal period and protecting agency, quantified the effects of slope, fuel moisture, weather, distance to water, and human exposure metrics on dispatch timing. Aircraft responded to 1,476 fires, with USFS aircraft having a slightly lower average response time. Hazard ratios indicated faster response times on wildfires under higher temperatures, and nearer populations, while wetter fuels and greener than average vegetation conditions delayed response. This study demonstrates the feasibility of real-time, cross-agency performance monitoring, informing resource allocation, and future integration of ADS-B with existing federal tracking systems for a comprehensive aviation situational awareness framework.

Introduction

Wildland firefighting agencies employ a diverse array of strategies and resources to combat wildfires, including the extensive use of aviation assets. Aerial resources, such as helicopters and air tankers, influence fire outcomes by delivering water, retardant, and personnel to locations in difficult terrain or areas with limited water access, while also providing critical intelligence to support decision-making on the ground. In California, two prominent agencies, the U.S. Forest Service (USFS) and California Department of Forestry and Fire Protection (CAL FIRE), manage significant aviation operations designed for wildfire response. Although CAL FIRE and the USFS are distinct organizations shaped by different mandates and missions, they are united by a shared responsibility for wildfire suppression and have legal agreements to work in coordination, particularly during the initial-response (IR) phase when aviation resources are rapidly mobilized (U.S. Forest Service, 2023; CAL FIRE, 2025). CAL FIRE and the U.S. Forest Service operate under reciprocal Direct Protection Area (DPA) arrangements in California, whereby either agency may hold primary suppression responsibility on state or federal lands, including some areas under federal jurisdiction (Pimlott, Laird and Brown Jr, 2015). Additionally, Region 5 of the USFS (which is comprised of the state of California) accounted for nearly a

quarter of all aviation flight hours contracted by the agency, further illustrating the high use of aerial firefighting support in California (U.S. Forest Service, 2021a).

During the IR phase of wildfire response, both CAL FIRE and the USFS prioritize rapid aircraft dispatch using the *closest resource concept*, ensuring the nearest available aircraft responds to a fire regardless of agency ownership (National Interagency Coordination Center (NICC), 2023). This cooperative approach enables the efficient use of limited aerial suppression assets across overlapping jurisdictions, particularly in California where state and federal responsibilities frequently intersect. Wildfire managers directly order aircraft from the administering airbase via intercom if the base is staffed; otherwise, they place requests through the Geographic Area Coordination Center (GACC), which manages aircraft availability and assignment statewide.

The importance of this coordinated aerial response became especially evident during California's 2020 wildfire season, one of the most destructive and costly on record (Safford *et al.*, 2022). Firefighting agencies in California responded to 8,648 wildfires, which collectively burned more than 4.3 million acres across the state, more than double the recent previous state-record and representing nearly 4 % of California's land area (Porter, Crowfoot and Newsom, 2020). Among these, the August Complex Fire became California's first officially recognized *gigafire*, burning more than 1 million acres across seven counties (Keeley and Syphard, 2021). The exceptional scale and intensity of these incidents placed demands on aerial resources, prompting both CAL FIRE and the U.S. Forest Service to heavily utilize aircraft to support suppression efforts across the state.

To meet these demands, CAL FIRE operates the largest civil aerial firefighting fleet in the world, as a component of its wildfire suppression program. The agency's aviation program includes a diverse array of aircraft designed to deliver rapid fire suppression in California's challenging and often extreme wildfire conditions. CAL FIRE manages its fleet of approximately 24 tankers, 25 helicopters, and 19 tactical aircraft from 14 strategically located air tanker bases across the state (CAL FIRE, 2025). In comparison, Region 5 (California) accounted for the highest level of Forest Service aviation activity nationwide, with 20,550 flight hours, representing 24.7% of all Forest Service aviation use and more than double any other region (U.S. Forest Service, 2021a). The regional fleet included a mix of contracted and agency-owned helicopters, fixed-wing aircraft, airtankers, and water scoopers that supported wildfire suppression and other mission needs. Of these, helicopters played a particularly critical role, reflecting the region's reliance on rapid aerial suppression in steep and inaccessible terrain. Across the Forest Service, aircraft delivered over 122 million gallons of liquid, of which more than 119 million gallons were water and 3.4 million gallons were retardant, with a significant share occurring in California due to the region's extensive fire activity. Region 5 airtanker operations totaled approximately 1,616 flight hours (17.1% of national airtanker time). Currently, the USFS tracks the application of these liquids using Automated Telemetry Unit (ATU) to document resource use (U.S. Forest Service, 2021b); however, comparable data for CAL FIRE operations are not publicly available, limiting direct comparisons between federal and state aerial suppression metrics.

No unified aviation dataset exists that captures cross-agency aircraft activity during wildfire response, preventing evaluation of statewide IR coordination. This lack of publicly accessible state-level aviation data underscores the value of leveraging independent, standardized tracking systems. Automatic Dependent Surveillance–Broadcast (ADS-B) technology, already mandated across most U.S. airspace, offers a solution by providing continuous, high-resolution data on aircraft location and movement (Varga, Polgár and Hedeşiu, 2015; Ali, 2016; Leonardi, 2018). Federal Aviation Administration (FAA) regulations mandate the use of ADS-B Out transmitters in most airspaces, enabling the monitoring of firefighting aircraft (Federal Aviation Administration,

2020). ADS-B technology has been successfully integrated into wildland fire operations to monitor unmanned aircraft systems (UAS) (Martin *et al.*, 2022; Bakowski *et al.*, 2024). It has also been used to analyze aerial firefighting operations, highlighting the effectiveness and cost-efficiency of different aircraft types based on mission patterns, deployment techniques, and resource delivery (Struminska and Filippone, 2024). Because ADS-B is present on all aircraft and the reporting is standardized across agencies, ADS-B technology offers a valuable opportunity to enhance the tracking and analysis of aviation operations, providing insights into state-managed aviation resources that can complement existing research focused primarily on USFS operations.

The goal of this study is to use ADS-B flight tracking data and survival analysis techniques to quantify differences in IR response times, operational patterns, resource deployment strategies, and fleet usage between agencies involved in aviation operations in California in 2020. By applying Aalen-Johansen estimators and using Cox proportional hazards modeling approaches, the study seeks to generate empirical timelines of aircraft response times for these agencies during the IA phase. In addition to characterizing response patterns, the analysis will explore how physical, biological, social, and administrative attributes, such as topography, vegetation characteristics, and population density, influence the likelihood that a wildfire receives an aerial response during the first 24 hours of ignition. Ultimately, the goal is to bridge methodological gaps between real-time aviation tracking and operational analysis, helping to inform more effective cross-agency coordination and aviation resource management strategies during wildfire suppression.

Methods and data:

Data Acquisition and Fleet Identification for CAL FIRE and USFS Aircraft

This study uses ADS-B data provided by the OpenSky Network to address gaps in understanding aviation activities during wildfire suppression efforts (Schäfer *et al.*, 2014). The OpenSky Network is a non-profit organization that offers open access to real-world air traffic control data collected through a global network of ADS-B and Mode S sensors. By providing detailed flight trajectories, timestamps, and aircraft identifiers, OpenSky enables comprehensive analysis of aerial firefighting operations, including flight patterns and suppressant delivery activity (Olive *et al.*, 2020; Magstadt *et al.*, 2024).

To evaluate aerial operations conducted by CAL FIRE and the USFS during the 2020 California wildfire season, all known firefighting aircraft were identified by tail numbers and cross-referenced with Federal Aviation Administration (FAA) registration data to confirm aircraft make, model, and associated ADS-B identifiers (https://registry.faa.gov/aircraftinquiry/search/nnumberinquiry). ADS-B flight records for these aircraft were collected from the OpenSky Network using a Python-based workflow that automated monthly data retrieval via the *pyopensky* package and a *Trino* query interface (Schäfer *et al.*, 2014; Sun *et al.*, 2019). Tail numbers were converted to their corresponding ICAO24 codes, which served as unique identifiers within the OpenSky database. Retrieved data were subsequently processed into GeoDataFrames for spatial and temporal analysis of aerial suppression activity.

We accessed NASADEM tiles through the Planetary Computer STAC API (NASA JPL, 2020), interpolated ground elevations at each aircraft location, and calculated height above ground level (AGL) by differencing geometric altitude from the surface elevation. Data were filtered to retain observations within a maximum 5000-meter AGL threshold to focus on operational flight segments relevant to wildfire suppression. Finally, monthly outputs were saved as shapefiles to analyze temporal patterns, deployment behaviors, and survival modeling. This approach enabled the construction of a detailed, elevation-corrected movement dataset across both agencies' aviation operations. The dataset spans January 2020 through December 2020 and includes high-resolution positional information (latitude, longitude, altitude, and timestamp) recorded at a 1-Hertz frequency (Figure 1). Data coverage is based on the OpenSky Network's ground-based sensor network, which exhibits geographically variable coverage due to terrain and sensor distribution (Strohmeier *et al.*, 2021).

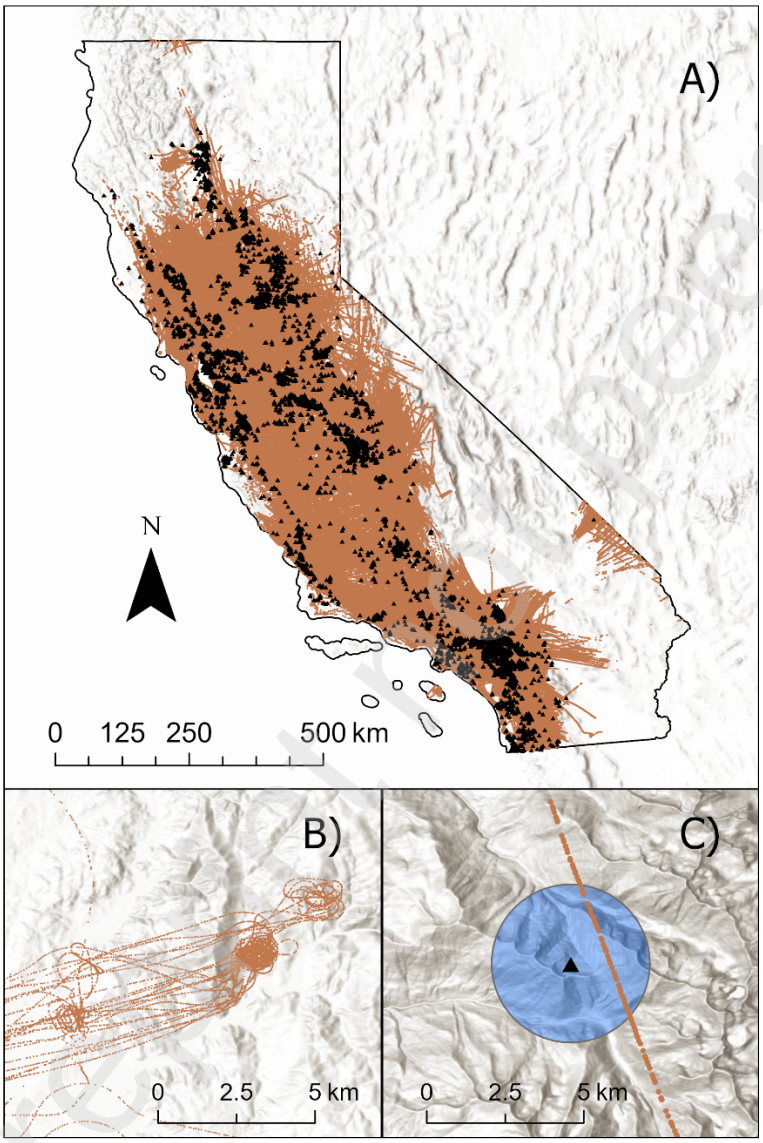

Figure 1. An overview of the study area (A), including aircraft flight paths derived from ADS-B data in orange and wildfire ignition points represented as triangles across California. Insets illustrate (B) aircraft circling patterns near active fires and (C) the 5 km detection radius used to assess aircraft arrival after ignition.

To examine CAL FIRE's aviation operations, the study focused on its permanently maintained, state-funded fleet, comprising 77 aircraft. As of 2025, this fleet included 25 Grumman S-2T airtankers, 7 Lockheed C-130H Hercules airtankers, 12 UH-1H Super Huey helicopters, 12 Sikorsky S-70i helicopters, 18 Rockwell OV-10 aircraft, and 2 King Air A200 aircraft (CAL FIRE, 2025). In contrast to CAL FIRE's permanent fleet model, the USFS relies on a dynamic combination of exclusive-use and call-when-needed contracts to secure its aerial firefighting resources. To focus specifically on aircraft capable of performing retardant drops, this study used ATU drop logs, which are required for all USFS-contracted aircraft capable of this operation, including airtankers and type one helicopters. Any aircraft that conducted at least one recorded retardant or water drop between 2017 and 2024 was included in the analysis. These aircraft were then cross-referenced with OpenSky ADS-B data to compile comprehensive flight histories. The USFS fleet identified in this dataset includes a range of helicopters and fixed-wing airtankers. Among the heavy-lift Type 1 helicopters, the most commonly used models included Boeing CH-47D, Sikorsky S-70i, Kaman K-1200, Sikorsky UH-60A, Sikorsky S-64E, and CH-54B helicopters. The mid-lift Type 2 helicopter fleet primarily included Bell UH-1H, Bell 205A-1, Airbus MBB-BK117 D-3, and Sikorsky S-58 variants. For fixed-wing airtankers, the USFS operated a variety of aircraft models including Bombardier DHC-8, Lockheed C-130, Boeing 737-3H4, McDonnell Douglas DC-9-87 and MD-87, British Aerospace AVRO 146-RJ85A and Bae 146, Bombardier CL-415, Canadair CL-215-6B11, and McDonnell Douglas DC-10. Overall, the USFS dataset captured four very large airtankers (VLATs), 48 large airtankers (LATs), 83 Type 1 helicopters, and 42 Type 2 helicopters actively engaged during the study period.

The USFS dataset covers helicopters and fixed-wing aircraft involved in wildfire suppression from 2017–2024, matching the full span of available ATU records. Because USFS helicopter ATU drop logs were anonymized, we did not have an exact year-by-year list of helicopters used; instead, we compiled a comprehensive 2017–2024 roster of USFS contracted aircraft and, for California, considered helicopters in-scope if they were wildland-mission capable, based in or regularly operating in the state, and had a plausible operational range for responding to California wildfires. Together with CAL FIRE, these datasets provide a detailed operational portrait of California's aerial firefighting and underpin our survival analyses.

Aviation Use Summary Statistics To complement the survival models, we developed a set of descriptive statistics that summarize aviation workload, response timing, and spatial deployment patterns for CAL FIRE and the USFS during the 2020 season. Using the full ADS-B dataset, we first calculated the number of unique active aircraft per day for each agency, producing a daily time series of fleet utilization. These daily activity profiles capture seasonal patterns in aircraft use and provide a baseline context for interpreting when each agency was most operationally engaged.

We then examined how proximity to airbases related to response outcomes by mapping all ignition points alongside airbase locations and classifying each fire by its first-arriving agency. For each ignition, we summarized response time metrics (mean, median, and percentile values), enabling a comparison of typical arrival times. Rather than relying solely on averages, we constructed empirical response-time distributions for both agencies to show how arrival times varied across the full IA window.

To assess spatial patterns of aviation activity, we rasterized all ADS-B flight trajectories to produce gridded density surfaces for CAL FIRE and USFS separately. Each raster records the cumulative number of aircraft-seconds per grid cell across the study period. We also generated

a difference surface (CAL FIRE minus USFS), which highlights areas where one agency operated more intensively than the other. This product provides a spatially explicit view of how aircraft from each agency used airspace over the course of the season and supports comparisons of regional deployment patterns.

Aircraft Response Timing to Initial Fire Discoveries

The OpenSky dataset provided timestamps, geographic positions, and unique aircraft identifiers (ICAO24 codes), which we processed to construct time series visualizations and to detect aircraft presence near wildfires. Wildfire occurrence data were obtained from the Fire Program Analysis Fire-Occurrence Database (Short, 2022), which includes discovery date, discovery time (HHMM format), fire size, and ignition coordinates. Of the 10,198 wildfires reported in California in 2020, 8,213 had valid discovery time and date information.

To calculate aviation response times, we spatially and temporally matched wildfire discovery records with ADS-B flight detections. Aircraft detections were filtered to those occurring within 5 km of a fire's ignition point and within 24 hours following its discovery. The 5-km radius was selected to accommodate the positional uncertainty of ignition records, which are typically reported at section-level accuracy, ensuring that aircraft detections are captured even when discovery coordinates are offset from the true ignition location. We defined initial response as the first 24 hours following discovery, consistent with federal guidance that treats this period as the typical length of the initial operational window before a fire transitions to extended response (Congressional Research Service, 2023). For each fire, response time was defined as the elapsed minutes between discovery and the first qualifying aircraft detection. As a sensitivity check, we repeated the analysis using alternative spatial thresholds of 7 km and 9 km; response time estimates were qualitatively similar across radii, indicating that results were not sensitive to the specific distance threshold chosen.

Fires with no recorded aircraft activity and no detections within this radius were excluded, as they likely occurred outside the effective surveillance range of the ADS-B network rather than reflecting a deliberate decision not to respond. This filtering step removed 1,003 fires from the dataset and ensures that subsequent analyses reflect operational patterns within the ADS-B–observable portion of the state.

Initial Response Analysis

The data was structured so that each row represented a single response time observation per fire. The reshaped datasets were concatenated, and for each fire, the minimum recorded response time across both agencies was selected to define the duration to first aircraft arrival. Each fire was assigned an event code: one if CAL FIRE arrived first, two if USFS arrived first. Fires without a recorded response within the observation window were right-censored by setting their duration to the maximum observed time (24 hours from ignition) and assigning an event code of zero.

The resulting dataset (FPA_ID, duration, event_type, Agency) was then used to fit a nonparametric competing risks model using the Aalen–Johansen estimator (Aalen and Johansen, 1978). For each unique event time, transition intensity matrices were constructed to represent the probability of transition into each of the two groups (CAL FIRE first, USFS first). These matrices were cumulatively multiplied to derive the cause-specific cumulative incidence functions (CIFs), which quantify the probability over time that each agency is the first to

respond. CIFs were then plotted to visualize how these probabilities evolve, appropriately accounting for the competing nature of response events and censoring. Unlike standard survival curves, CIFs account for the fact that multiple outcomes can prevent the occurrence of one another, in this case, the arrival of one agency precludes the other from arriving first.

While the competing risks model identifies which agency is more likely to arrive first, it does not examine the factors influencing response timing. To study the influence of landscape, weather, and operational conditions on aircraft arrival, we applied a Cox proportional hazards model (Cox, 1972). Using the same fire-level dataset, we kept each fire's observed duration and flagged the event indicator as 1 when an aircraft from either agency arrived and 0 when no aircraft arrived within 24 hours. The model was fitted using the Breslow method for baseline hazard estimation and standard errors (Breslow, 1974). Estimated hazard ratios represent the multiplicative effect of each covariate on the instantaneous rate of aircraft arrival, holding other variables constant. Model fit and proportional hazards assumptions were assessed using the Schoenfeld residual-based diagnostics (Schoenfeld, 1982).

We estimated three separate Cox proportional hazards models. Each model incorporated the same covariates but differed in stratification approach. In the first model, we included no stratification to provide a baseline specification. The second model added fixed effects stratified by time of day, derived from the fire discovery time (DISCOVERY_TIME), based on prior evidence that large airtanker activity peaks during afternoon hours when fire behavior typically intensifies (Thompson *et al.*, 2018; Reinke *et al.*, 2021). Fires were categorized into three periods based on local discovery hour: Morning (06:00–12:59), Afternoon (13:00–20:59), and Night (21:00–05:59). This classification allowed us to account for operational rhythms and diurnal variation in fire behavior and aircraft dispatch likelihood. The third model introduced stratification by DPA, which delineates zones of primary suppression responsibility across federal, state, and local fire agencies, to account for differences in fire management arrangements, resource availability, and dispatch practices across protection zones. This stratified modeling framework allowed us to evaluate the stability of covariate effects while accounting for temporal and jurisdictional heterogeneity in aerial response behavior.

Covariate Selection

Vegetation and fuel characteristics have been shown to affect airtanker use and deployment patterns (Stonesifer et al., 2016), making vegetation and fuel characteristics an important factor for modeling aerial suppression decisions. To characterize live fuel conditions consistently across California's diverse ecosystems, we used the Normalized Difference Vegetation Index (NDVI), which provides continuous spatial coverage and reflects live photosynthetic activity across forested, shrubland, grassland, and developed environments (Pourmohamad *et al.*, 2023). NDVI captures short-term variability in vegetation greenness that can influence ignition potential, flame intensity, and tactical considerations during the IR phase. Because vegetation stress typically appears as reduced greenness, negative NDVI anomalies, departures below a site's recent mean, have been linked to elevated wildfire potential (Burgan, 1996; Chuvieco et al., 2004; Sall, Jenkins and Pushnik, 2013).

We therefore derived a standardized day-prior NDVI anomaly (NDVI_ANOM) for each fire using the following formulation:

$$NDVI_{ANOM} = \frac{NDVI_{d-1} - NDVI_{mean,m}}{(NDVI_{max,m} - NDVI_{min,m})/4}$$

where $NDVI_{d-1}$ is the NDVI on the day before discovery, and $NDVI_{mean,m}$, $NDVI_{max,m}$, and $NDVI_{min,m}$ are the mean, maximum, and minimum NDVI values for the corresponding calendar month over the preceding 12 months. We scaled anomalies by dividing the month-specific NDVI range $(NDVI_{max,m} - NDVI_{min,m})/4$, where the range is computed from the same calendar month over the preceding 12 months. This anomaly highlights departures from expected seasonal conditions, offering an indicator of live-fuel conditions that can shape how aircraft are used during initial response. Because unusually low NDVI anomalies signal stressed, more flammable live fuels, they also serve as a proxy for conditions under which initial response is more difficult to contain with ground resources.

To complement the live-fuel signal provided by NDVI, we included 100-hour dead fuel moisture (fm100) as a measure of background fuel aridity, a variable that strongly influences fire behavior and is a component of fire danger rating systems (Andrews, Loftsgaarden and Bradshaw, 2003; Jolly *et al.*, 2024). Not only does it strongly influence fire behavior, lower dead-fuel moisture increases the likelihood of ignition, rate of spread, and fireline intensity; 100-hour fuel moisture is also an input to operational fire-behavior models, underscoring its importance (Rothermel, 1986).

Topographic constraints were represented using slope steepness from LANDFIRE terrain data. Steeper slopes can limit ground access, reduce handline effectiveness, and increase reliance on aerial resources (Thompson et al., 2018; Wheatley et al., 2022). Additionally, steep slopes tend to elevate firefighter risk by increasing flame exposure, entrapment potential, and the difficulty of safe escape route construction, conditions that often require greater suppression (Page and Butler, 2018).

Weather-driven fire danger was characterized using wind speed at 10 m (vs), maximum temperature (tmmx), and the Burning Index (bi), all from GridMET (Abatzoglou, 2013). These variables capture environmental conditions that are closely associated with periods of intensified fire behavior and increased demand for aerial support (Thompson et al., 2018; Wheatley et al., 2022; Simpson et al., 2022). Because weather is one of the primary situational cues used by incident commanders, these factors are often incorporated, consciously or intuitively, into assessments of potential fire behavior and suppression needs (Thompson and Calkin, 2011). Together, these weather variables provide a dynamic representation of conditions that influence both fire growth and the likelihood of early aircraft deployment.

Operational logistics were represented through distance to water bodies (dist_to_water_km), used as a proxy for dip-site availability. Proximity to suitable water sources has been shown to influence both airtanker and helicopter deployment patterns (Plucinski, 2025), making it an important consideration for IR response.

Finally, values-at-risk covariates were included to capture the influence of human exposure on aerial suppression decisions. The Global Human Modification Index (GHM) and 1-km population density (Popo_1km) from WorldPop were used to represent development pressure and

wildland–urban interface proximity, consistent with findings that aircraft deployments often concentrate near populated areas (Stonesifer et al., 2016).

With the exception of distance to water sources, all covariates were sourced from the FPA FOD-Attributes dataset (Pourmohamad et al., 2023). Table 1 provides the full list of variables, definitions, and data sources.

Table 1.Covariate names, descriptions, and data sources used in the survival analysis of aerial initial response.

Variable Name	Description	Source
fm100	100-hour dead fuel moisture (%)	(Abatzoglou, 2013)
NDVI_ANOM	Standardized day-prior NDVI anomaly computed from four components (day-prior NDVI, and monthly mean, maximum, and minimum NDVI over the preceding 12 months)	(Vermote, 2019; Pourmohamad *et al.*, 2023)
Slope	0-90 degrees	(Rollins, 2009)
dist_to_water_km	Distance to nearest waterbody (km)	(California Department of Fish and Wildlife, 2025)
vs	Wind velocity at 10 m above ground (m/s)	(Abatzoglou, 2013)
bi	Burning index (NFDRS fire danger index)	(Abatzoglou, 2013)
tmmx	Maximum temperature (K)	(Abatzoglou, 2013)
GHM	Cumulative measure of the human modification of lands within 1 km of the fire ignition point	(Kennedy *et al.*, 2019)
Popo_1km	Average population density within a 1 km radius around the fire ignition point	(WorldPop and CIESIN, 2018)

Results:

Aircraft activity and Seasonal Patterns

We obtained 17,884,545 positional records (≈4,968 flight hours) for USFS aircraft and 21,925,926 records (≈6,090 hours) for CAL FIRE aircraft, representing second-by-second tracking across the 2020 season where ADS-B data was available. CAL FIRE activity (Figure 2, top) increased through the summer, peaked in September, and declined in November. USFS aircraft showed a broadly similar seasonal pattern but with a slightly later and more diffuse peak and fewer individual aircraft active on a typical day (Figure 2, bottom).

.

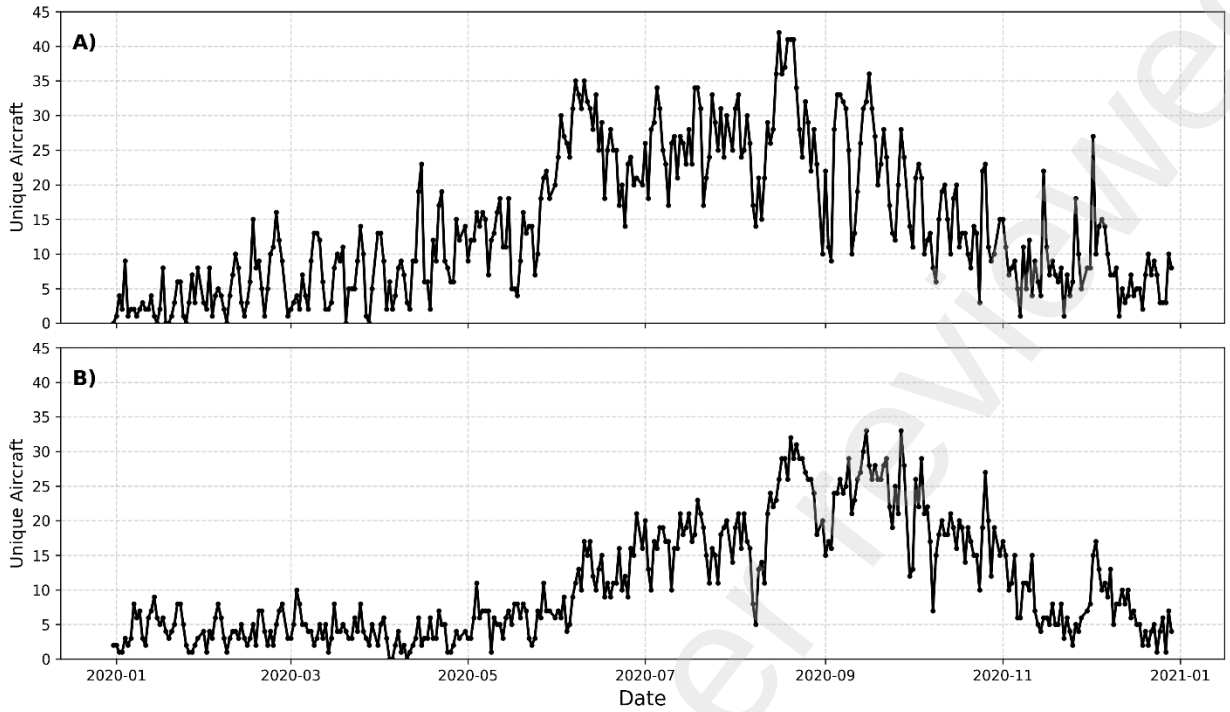

Figure 2. Line plot illustrating the distribution of unique aircraft activities (CAL FIRE top, USFS bottom) by day for 2020.

To compare spatial patterns of airspace use, we generated a density-difference surface representing USFS aircraft density minus CAL FIRE aircraft density at a 3-kilometer resolution (Figure A1). Positive values indicating areas more frequently traversed by USFS aircraft and negative values indicating higher CAL FIRE activity. The map shows dense flight-path corridors and incident hubs across the state, with pockets of higher CAL FIRE activity indicated by dark purple values and pockets of higher USFS activity indicated by bright yellow values.

Incident Summary and Response Times

A total of 7,214 wildfire incidents were included in the analysis. Of these, 1,476 received an aerial response within 24 hours of discovery (840 CAL FIRE, 637 USFS), while 5,737 had no recorded aerial response and were classified as “NoResponse.” Response times were right-censored at 1,440 minutes (24 hours). Among incidents with a recorded response, CAL FIRE arrival times averaged 700 minutes (median 751; IQR: 387–1007), and USFS arrival times averaged 673 minutes (median 680; IQR: 406–962). Fifty-five incidents had an initial response within 20 minutes (37 CAL FIRE, 18 USFS).

Proximity to Airbases

Distances from ignition points to the nearest CAL FIRE airbase ranged from about 0.25 to 254 km across all fires (Figure A2). Mean distances were 33.5 km for CAL FIRE-first responses (n = 840), 35.6 km for USFS-first responses (n = 637), and 46.9 km for NoResponse fires (n = 5,737). Medians showed a similar pattern: 29.7 km (CAL FIRE-first), 35.4 km (USFS-first), and 42.7 km (NoResponse). Although the distributions overlapped across response types, fires that received an initial aerial response were generally closer to an airbase, while NoResponse fires exhibited both the largest mean and median distances.

Across all three panels in Figure 3, ignition locations are distributed statewide with a broad north–south pattern along the Sierra Nevada, Coast Range, and southern California foothills. NoResponse fires (Panel A) are widely dispersed across the same areas where responded fires occur. CAL FIRE-first responses (Panel B) and USFS-first responses (Panel C) show overlapping geographic footprints, with both agencies' initial responses appearing throughout northern, central, and southern California. CAL FIRE airbases (triangles) are positioned across the state, and incidents of each response type occur in proximity to multiple bases rather than clustering around any single region.

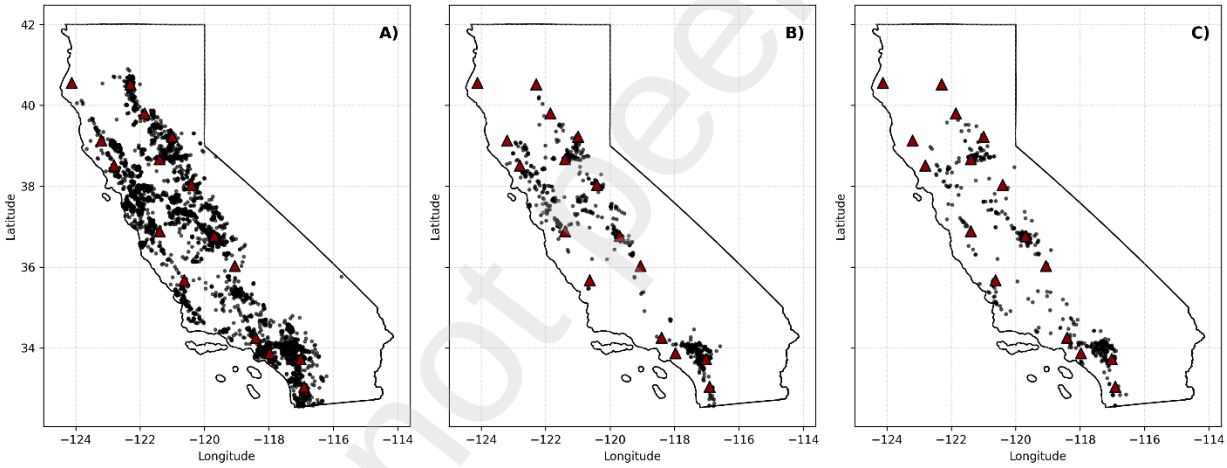

Figure 3. Spatial distribution of fire response types and CAL FIRE airbases across California. Panels show (A) incidents with no aerial response, (B) incidents where CAL FIRE aircraft responded first, and (C) incidents where USFS aircraft responded first. Black points represent incident locations, and red triangles indicate airbase locations.

NDVI Results

Across all 7,214 fires, standardized day-prior NDVI anomalies (NDVI_ANOM) ranged from roughly –8 to +5, with most values falling between –2 and +2 and a slight tendency toward more negative anomalies during the core 2020 fire season (Figure A3). When grouped by event type, NDVI_ANOM distributions for fires that received no aircraft and those that received an aerial response were broadly similar, with medians near zero and strongly overlapping interquartile ranges (Figure A4). In the Cox models, however, NDVI_ANOM consistently had a negative and highly significant coefficient ($\beta \approx -0.10$, $p < 0.001$ in all three specifications; Table 2), indicating that, after accounting for fuel, weather, exposure, and distance-to-water covariates, increasingly

positive NDVI anomalies were associated with lower estimated hazards of aircraft arrival and increasingly negative anomalies with higher hazards.

Cumulative Incidence of First Response

Cause-specific cumulative incidence functions (Figure 4) show the probability of each agency being first to arrive over time. By 1,440 minutes, the cumulative incidence reached approximately 0.12 for CAL FIRE and 0.09 for USFS. Confidence intervals (shaded bands) reflect uncertainty around each estimate.

Cox Proportional Hazards Models

We estimated three Cox proportional hazards models: (1) an unstratified baseline model, (2) a model stratified by discovery time (Morning/Afternoon/Night), and (3) a model stratified by DPA region (Table 2). Schoenfeld residual diagnostics are provided in Appendix A5, and robustness checks excluding covariate groups are shown in Appendix Table A6.

Across all three Cox model specifications, coefficient signs and magnitudes were consistent (Table 2). Maximum temperature (tmmx), nearby population density (Popo_1km), and human-modified landscape values (GHM) had positive coefficients in every model, indicating higher estimated hazards of aircraft arrival when increased. NDVI_ANOM, distance to water, and fm100 had negative coefficients across models. Slope, wind speed (vs), and burning index (bi) showed coefficients near zero with no meaningful variation across specifications. Effect sizes for the major covariates were stable across Models 1–3, and no coefficient changed sign between models. The time-of-day–stratified model produced the lowest BIC value, indicating slightly better fit relative to the baseline and DPA-stratified models. Hazard ratios and confidence intervals from all three model specifications are shown in Figure A7.

The baseline survival functions for the DPA-stratified model (Model 3) differed across the three DPA groups (Figure 5). STATE-managed fires (n = 2,006) showed the steepest decline in survival probability over the 24-hour window, indicating a higher baseline hazard of aircraft arrival under this stratification. LOCAL DPAs (n = 5,088) exhibited the slowest decline, maintaining the highest survival probabilities for most of the time range. FEDERAL DPAs (n = 120) showed an intermediate trajectory, though the curve displayed more irregular step patterns compared to the other groups, reflecting the smaller sample size for FEDERAL-managed fires. All curves steadily decreased, consistent with the accumulation of aircraft arrival events over the observation period

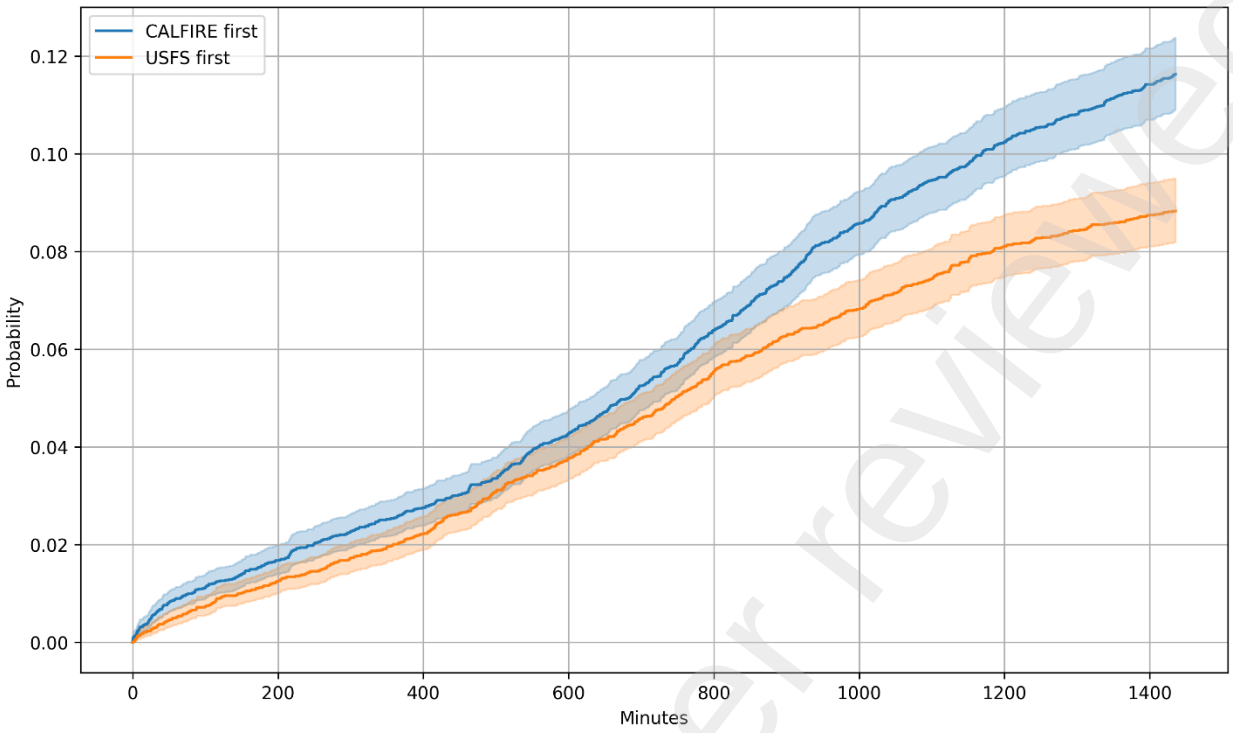

Figure 4. Cumulative incidence functions (CIFs) estimated using the Aalen–Johansen method for initial aircraft response to wildfires in California during 2020. The blue line represents the probability over time that CAL FIRE is the first to respond; the orange line represents USFS. Shaded areas indicate 95% confidence intervals. Time is measured in minutes from fire discovery.

*Table 2. Coefficient estimates and standard errors from three Cox proportional hazards models examining factors associated with time to initial aircraft arrival on wildfires in California during the 2020 fire season. All models include the same covariates with Model 1 (unstratified), Model 2 (stratified by time of day), and Model 3 (stratified by DPA). Values represent log hazard coefficients; standard errors are in parentheses. Positive coefficients indicate factors associated with faster aircraft dispatch. Statistically significant effects are denoted by conventional markers (*p < 0.05; **p < 0.01; ***p < 0.001; +p < 0.10). Each model includes 7,214 wildfire events.*

	Model 1	Model 2 (Time strata)	Model 3 (DPA strata)
fm100_z	-0.074 (0.054)	-0.078 (0.054)	-0.064 (0.054)
NDVI_ANOM_z	-0.100*** (0.024)	-0.101*** (0.024)	-0.099*** (0.024)
Slope_z	0.043 (0.031)	0.043 (0.031)	0.008 (0.035)
dist_to_water_km_log_z	-0.060* (0.026)	-0.060* (0.026)	-0.037 (0.027)
vs_z	-0.056 (0.041)	-0.056 (0.041)	-0.053 (0.040)
bi_z	0.044 (0.058)	0.038 (0.058)	0.049 (0.058)
tmmx_z	0.448*** (0.038)	0.445*** (0.038)	0.464*** (0.038)
GHM_z	0.119* (0.051)	0.117* (0.051)	0.193*** (0.054)
Popo_1km_log_z	0.146** (0.047)	0.148** (0.047)	0.166*** (0.048)
Num.Obs.	7214	7214	7214
BIC	25567.6	22441.0	23740.2

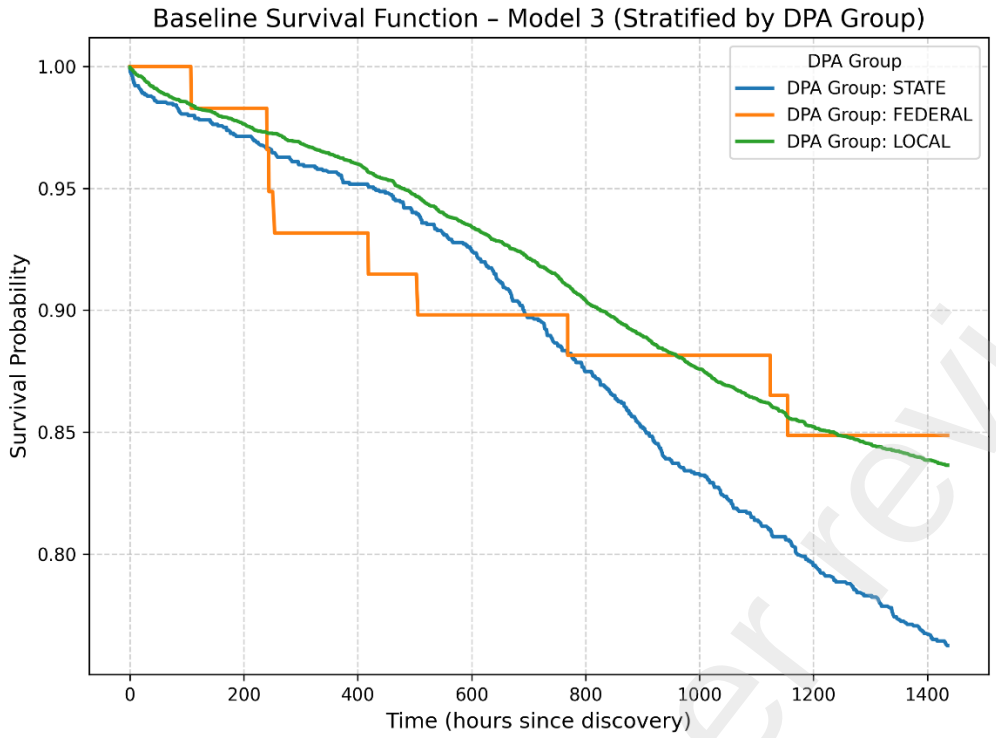

Figure 5. Baseline survival functions from the DPA-stratified Cox model (Model 3). Curves show the estimated probability that no aircraft has arrived as a function of time since fire discovery for STATE, FEDERAL, and LOCAL Direct Protection Areas.

Discussion

The cause-specific cumulative incidence curves rise steadily rather than showing an early step change, indicating that the probability of receiving an aircraft is relatively diffuse across the first 24 hours during the IR phase (FIGURE 4). If aircraft were commonly launched immediately at discovery, we would expect a sharp initial jump; instead, both agencies exhibit a near-linear accumulation, with only a small fraction of fires receiving aircraft in the first 20 minutes. This pattern is consistent with the absence of any single, predictable “clock” governing when aircraft are dispatched after a fire’s discovery.

Responding to wildfire involves balancing multiple, sometimes competing priorities, including firefighter safety, suppression costs, public expectations, and the anticipated ecological outcomes of different response strategies, among others, which together shape when and how resources are deployed (Taber, Elenz and Langowski, 2013; Fillmore *et al.*, 2024). As a result, the timing of aerial response reflects the combined influence of fuel moisture, weather, slope, access to water, proximity to people and infrastructure, and the evolving fire situation, factors that seldom align uniformly across incidents. Operationally, dispatch is also mediated by availability (what’s on base, what’s already committed), airspace and smoke constraints, and maybe most importantly, human decision-making under uncertainty (Thompson and Calkin, 2011). That last element introduces real variability. Incident commanders weigh consequences, alternatives (ground attack, wait for IR/size-up), and risk thresholds differently, so two similar ignitions may lead to different call-up times. Together, these environmental, logistical, and human factors produce a broadly increasing, rather than front-loaded, arrival profile, with

modest early responses and a persistent chance of first arrival throughout the IA window. Practically, this means that improving situational awareness, coordination, and decision support tools may do more to contribute to timely and effective aerial response than any single operational change alone.

Building on this broader understanding of how response decisions unfold, the modeled results further show that aircraft are more likely to be mobilized under conditions of higher temperatures, patterns consistent with prior studies of aerial suppression behavior (Stonesifer *et al.*, 2016; Thompson *et al.*, 2018). This suggests weather, and more specifically hotter temperatures, may influence dispatch decisions. Wind speed, by contrast, had a small negative but statistically non-significant effect on the hazard of aircraft arrival, indicating no clear evidence that stronger winds systematically accelerate or delay aerial response in this dataset. This is consistent with operational practice, where incident commanders will still launch aircraft across a wide range of wind speeds when safety envelopes allow, even though higher winds are known to reduce drop effectiveness by increasing drift and making it harder for water or retardant to reach the target fuels (Fogarty and Slijepcevic, 1998). Additioally, steep terrain has historically been a focal point for retardant operations, our models show no statistically significant association between slope and the hazard of aircraft arrival (Thompson *et al.*, 2018). This may reflect either genuinely weak slope sensitivity in IA decision-making or the fact that ADS-B coverage is concentrated in lower-elevation terrain where slope variation is smaller and operational patterns differ from high-slope wilderness settings.

These same terrain- and weather-driven challenges also intersect with logistical considerations such as access to water. In our results, the distance-to-water term does not exhibit a consistently strong signal, suggesting that water availability may influence aviation use in some contexts but not uniformly across incidents. Several factors could explain this muted relationship. In remote areas where accessible water sources are scarce, longer ferry distances and fewer dip sites can constrain operations and shift reliance toward ground-based tactics (Keating *et al.*, 2012). Distance to water may also shape the type of aircraft used, the feasibility of placing water or retardant drops, and broader suppression strategies, but these influences may not manifest as a simple, statewide pattern.

Beyond logistics, distance to water is correlated with environmental characteristics that vary substantially across California’s landscapes. Fires farther from water often occur in settings with lower fuel continuity or reduced vegetation productivity, where aerial support may offer limited marginal benefit compared to ground attack. For example, (McNorton and Di Giuseppe, 2024) note that ecosystems with lower net primary productivity, common in arid regions distant from riparian areas, tend to have sparser or more discontinuous fuels, which constrain fire growth potential and may reduce the need for intensive aerial suppression. Thus, the weak statistical relationship observed here may reflect the combined influence of operational constraints, longer ferry distances, ecological gradients, and differences in fuel structure rather than a direct, statewide effect of water proximity alone.

Across all three Cox models, the NDVI anomaly term (NDVI_ANOM) is negative and highly significant, indicating that live-fuel conditions exert a consistent influence on whether aircraft are dispatched quickly. Because the anomaly was constructed so that negative values represent below-normal greenness for that location and month (drier, more stressed live fuels) and positive values represent greener-than-usual conditions, the negative coefficient means that fires igniting under more stressed vegetation are more likely to receive aircraft earlier. In

standardized units, a one–standard deviation increase in NDVI_ANOM (toward greener-than-expected vegetation) reduces the likelihood of aircraft arrival by roughly 10%, whereas a one–standard deviation shift toward more negative anomalies increases the likelihood of using aircraft. This pattern is consistent with prior work showing that NDVI anomalies and departures from “normal” greenness track live fuel moisture and elevated fire potential (Burgan, 1996; Chuvieco et al., 2004; Sall, Jenkins and Pushnik, 2013) and with recent efforts to incorporate improved live-fuel moisture representations into fire danger systems (Jolly *et al.*, 2024). Together, these results suggest that incident commanders are more inclined to mobilize aircraft under conditions when live fuels appear unusually dry for the season, not just when background dead fuels are dry, and that NDVI-derived indicators provide information about response decisions beyond what is captured by fm100 or composite fire-danger indices alone. This emphasis on anomalously dry fuels aligns with broader evidence from the 2020 season that unusual fuel conditions contributed to concerns about late-season large-fire potential and shaped strategic planning for suppression capacity (Belval et al., 2022).

While these environmental and logistical factors help explain where aircraft are less likely to be deployed, human and social factors appear equally important in determining where they are. Aviation deployments during initial response tend to intensify where high value property are at stake (Bayham and Yoder, 2020). Our model reproduces this pattern through positive coefficients on both the GHM and Popo_1km. Multiple empirical studies indicate that proximity to people and property is a strong driver of aerial-suppression decisions. A nationwide analysis of large-air-tanker missions during 2010–2014 showed that aviation assets were disproportionately concentrated within about 10 km of the wildland–urban interface, where population density and infrastructure are highest (Stonesifer *et al.*, 2016). A more detailed review of 2012 operations in Montana found the median distance from drop locations to mapped WUI values was only 2.8 mi, underscoring how protection of communities shapes deployment patterns (Stonesifer *et al.*, 2015). Consistent with these case studies, the U.S. Forest Service’s Aerial Firefighting Use and Effectiveness (AFUE) program reported that most drops across all aircraft types occurred on fires where values were threatened during the event, signaling that resource-at-risk considerations routinely influence aviation tasking at the national scale (U.S. Department of Agriculture, Forest Service, 2020). Taken together with our findings, these studies reinforce that aircraft are preferentially mobilized when fires threaten concentrated assets, whether homes or infrastructure, explaining the strong population-proximity signal in our hazard models.

While these results capture genuine operational behavior, they also reflect the spatial and technical constraints of ADS-B data. Line-of-sight reception means that ground-based ADS-B networks provide denser coverage in populated corridors and lower-elevation valleys, especially the Central Valley and Sierra foothills, while reception drops off in remote, mountainous regions such as far-northern coastal California, the high Sierra, and the southeastern deserts. To avoid conflating absent detections with absent response, we excluded 1,003 fires with no ADS-B messages within 5 km in 2020; however, this necessary filter shifts the analytic sample toward areas with robust sensor coverage, greater airbase density, and higher WUI exposure. Consequently, the estimated probabilities and timing of aerial response may be somewhat upward-biased relative to true statewide patterns, and differences between agencies may be muted if one agency more frequently serves wilderness and high-elevation terrain. Our findings should therefore be interpreted as describing IR activity that is observable via ADS-B, rather than representing all IR operations statewide. Future work could reduce these gaps by

incorporating satellite-based ADS-B reception or by outfitting aircraft with onboard, internet-connected systems capable of relaying position data in real time.

Despite these coverage limitations, ADS-B nevertheless provides a uniquely comprehensive view of aerial activity compared with traditional data sources. Existing wildfire aviation studies have relied primarily on ATU drop logs, which are mandatory for federally contracted airtankers but not for state fleets such as CAL FIRE. As a result, analyses using only ATU data (e.g., (Stonesifer *et al.*, 2022; Bayham and Bryan, 2023)) omit substantial portions of aerial suppression performed by state and private aircraft. ADS-B addresses much of this limitation, because all transponder-equipped aircraft broadcast their position every second, open networks like the OpenSky Network provide ownership-agnostic, continuous records of aircraft movement. Prior work has already shown that straightforward pattern-recognition methods applied to ADS-B tracks can identify CAL FIRE airtankers, map circling orbits over active fires, and reconstruct operational timelines without access to mission logs (Olive *et al.*, 2020).

ADS-B's strengths stem from its open broadcast architecture; low-cost receivers can collect signals wherever line-of-sight exists, and community archives now contain billions of messages (Schafer *et al.*, 2016). When integrated with incident records or the subset of federal ATU drops, these data support new spatial analyses of fleet utilization. Yet the system remains incomplete: coverage is uneven, mountainous terrain can obscure reception, and some aircraft still operate without broadcasting ADS-B even within mandated airspace. Advancing wildfire aviation research will therefore require hybrid data systems that merge terrestrial and satellite ADS-B, agency-specific telemetry, and emerging unmanned-aircraft sensors. Such integration would produce a more comprehensive and resilient picture of aerial firefighting activity and extend performance analyses beyond federal fleets to the state and local resources that increasingly shoulder IR responsibilities.

Conclusion

Figure 3 shows that the spatial distribution of response types is broadly consistent across California, with no discernible geographic clustering that would indicate systematic spatial bias in whether CAL FIRE or the USFS responds first. Incidents with no aerial response, CAL FIRE–first responses, and USFS–first responses all occupy the same statewide footprint, which aligns with the fact that CAL FIRE airbases are strategically located to provide wide and relatively uniform coverage. Because the airbase network is intentionally designed to minimize spatial gaps, a strong geographic signature in response patterns is not expected. The violin plot (Figure A2) shows a slight tendency for incidents receiving an initial aerial response to occur at somewhat shorter distances from CAL FIRE airbases compared with no-response incidents. This weak proximity signal is operationally intuitive, closer fires are more likely to receive aircraft simply because travel times are shorter and aircraft can be committed more efficiently. Overall, proximity to airbases appears to play a modest role in shaping response likelihood and sequencing, but it does not produce a pronounced spatial pattern across the state.

The results of this study indicate a cooperative balance in aviation workload between CAL FIRE and the U.S. Forest Service, reflecting the intertwined responsibilities defined under California's Direct Protection Area agreements. Despite differences in fleet composition and mission scope, the expected response times for the two agencies are nearly identical within the ADS-B–

observable portion of the state (Figure A8). This similarity suggests that, operationally, both agencies are contributing comparably to IR aviation response during high-activity periods.

Workload patterns further reinforce this shared commitment. The seasonal activity curves for the two fleets exhibit a nearly unimodal, parallel structure, with both agencies showing a midsummer–early fall pulse in aircraft activity (Figure 2). The similarity in these seasonal pulses indicates that both fleets scaled up and sustained aviation effort during the same fire-season periods, consistent with coordinated IR responsibilities. Spatial patterns also suggest a roughly even division of effort: the distribution of incidents first reached by each agency (Figure 3) shows substantial geographic overlap, rather than a clear partitioning of responsibility.

This balanced pattern of effort and engagement aligns with prior work documenting shared federal–state response structures and cooperative aviation management under DPA agreements and closest-resource dispatch protocols (NICC, 2023; U.S. Forest Service, 2023). It is also consistent with findings from Stonesifer et al. (2016), who showed that large airtanker use is requested at the incident level through a national dispatch system and is concentrated near populated areas, indicating that deployments are driven by operational needs and proximity to values at risk rather than purely by jurisdictional boundaries. Together, these results suggest that the combined CAL FIRE and USFS aviation systems operate less as two separate fleets than as a jointly involved suppression network responding to similar environmental triggers and workload pressures.

This study demonstrates that ADS-B's global, second-by-second telemetry provides a uniquely comprehensive lens on wildfire aviation use, allowing us to quantify when, where, and under what conditions CAL FIRE and USFS aircraft launch during initial response, something that has not been possible with traditional, agency-specific records. By linking aircraft trajectories with survival analysis, we show how terrain, weather, water access, and values-at-risk shape deployment timing and reveal patterns that were previously obscured by fragmented reporting systems. Rather than comparing agencies per se, our analysis illustrates how a unified, ownership-agnostic data stream can illustrate the broader operational environment in which both systems operate. As ADS-B continues to expand, further integration with federal and state tracking systems, shared data protocols, and more consistent coverage will strengthen its potential as the foundation for real-time coordination, performance assessment, and long-term planning. Together, these advances point toward a future in which a consolidated monitoring architecture supports more transparent, equitable, and strategically informed use of aviation resources during wildfire response.

Appendix

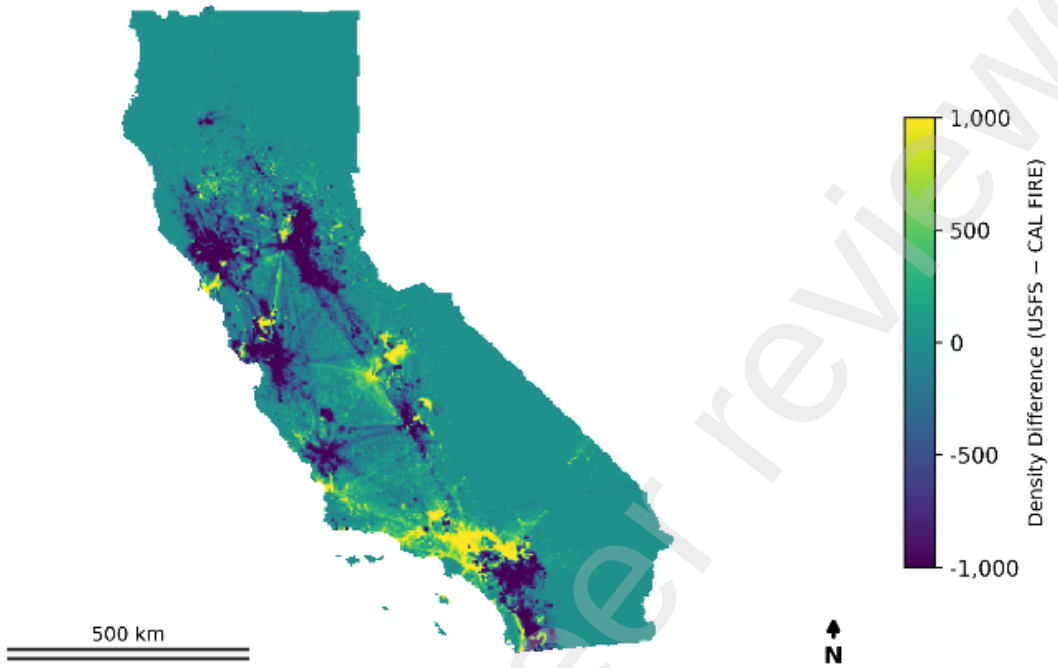

Figure A1. Difference in ADS-B–derived aircraft density between USFS and CAL FIRE aircraft across California during the 2020 fire season. Values represent USFS minus CAL FIRE cumulative aircraft-seconds per 3-km grid cell, with bright yellow areas indicating more frequent USFS use and dark purple areas indicating more frequent CAL FIRE use.

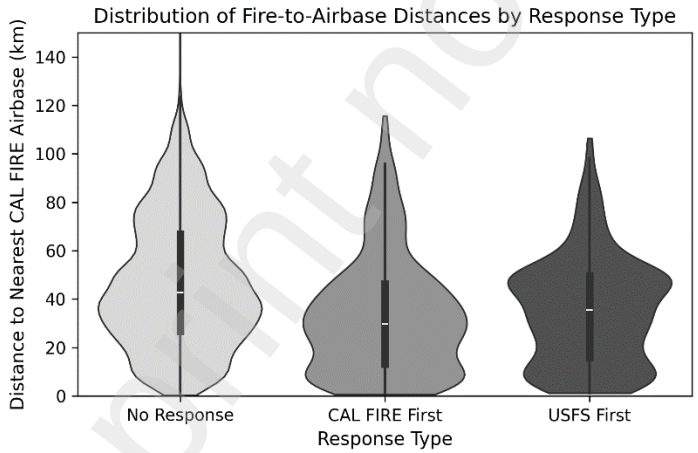

Figure A2. Violin plots showing distances from fires to the nearest CAL FIRE airbase, grouped by response type (No Response, CAL FIRE first, USFS first).

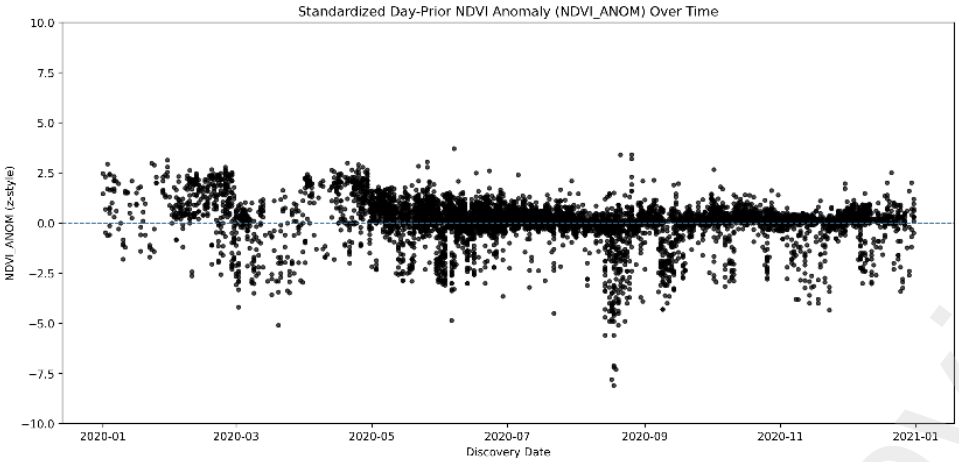

Figure A3. Standardized day-prior NDVI anomalies for all 2020 fires, showing departures from typical monthly greenness conditions over the fire season.

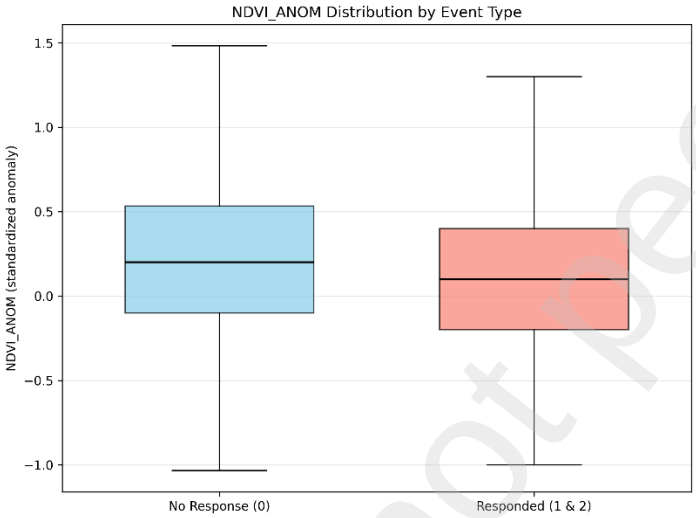

Figure A4. Boxplots comparing standardized NDVI anomalies for fires with no aerial response versus those that received an initial aircraft response.

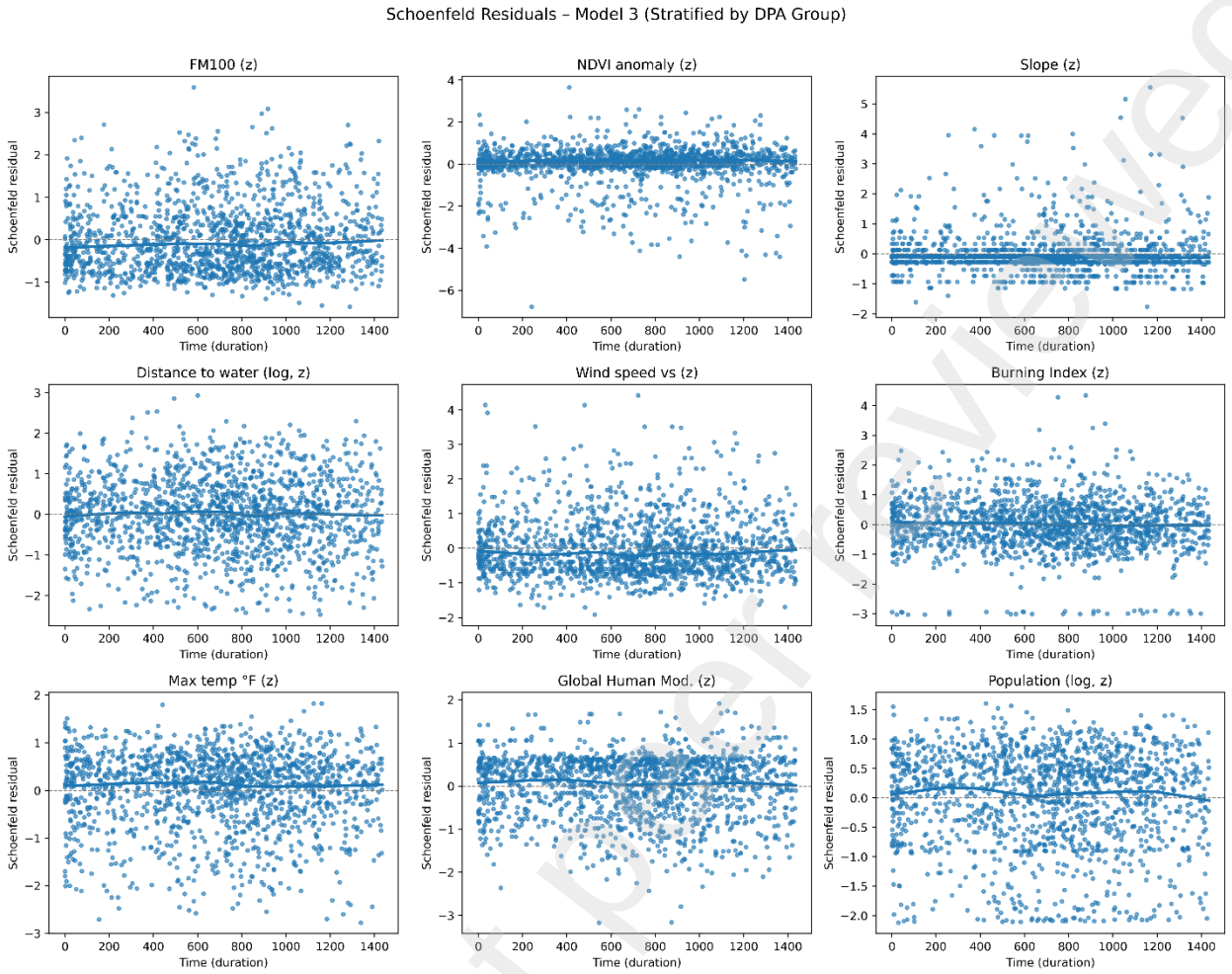

Figure A5. Shoenfeld residuals for model 1 used to assess the proportional hazards assumption of the dataset.

We evaluated the proportional hazards assumption of the Cox regression models using Schoenfeld residuals, visualized via the CoxPHFitter function in the lifelines library. These plots assess whether residuals remain independent of time, a key requirement for the validity of proportional hazards modeling. As shown in Appendix Figure A1, most covariates exhibit residuals that fluctuate randomly around zero, suggesting reasonable adherence to the assumption. Although formal statistical tests flagged minor violations for some covariates, these are likely artifacts of the large sample size or the continuous nature of the predictors rather than substantive departures from proportionality (Grambsch and Therneau, 1994). Given the stability of effect estimates across stratified model specifications and the lack of strong temporal patterns in residuals, we interpret the models as appropriately specified for estimating how landscape, weather, and exposure factors influence aircraft dispatch timing during the initial response phase.

Table A6. Robustness checks for Cox PH regression results.

	Full	No_Slope	No_Pop	No_Fuel	No_Weather
GHM	0.892*** (0.193)	0.799*** (0.178)	nan	0.861*** (0.192)	0.986*** (0.193)
NDVI_ANOM	-0.097*** (0.025)	-0.098*** (0.025)	-0.090*** (0.025)	nan	-0.108*** (0.025)
Popo_1km	0.006+ (0.004)	0.007+ (0.004)	nan	0.006 (0.004)	0.007+ (0.004)
Slope	0.009 (0.007)	nan	-0.015* (0.006)	0.009 (0.007)	0.003 (0.007)
bi	0.003 (0.003)	0.003 (0.003)	0.004 (0.003)	0.006** (0.002)	nan
dist_to_water_km	-0.034** (0.011)	-0.035** (0.011)	-0.039*** (0.011)	-0.036** (0.011)	-0.031** (0.011)
fm100	-0.021 (0.015)	-0.021 (0.015)	-0.003 (0.015)	nan	-0.109*** (0.009)
tmmx	0.034*** (0.003)	0.034*** (0.003)	0.035*** (0.003)	0.036*** (0.003)	nan
vs	-0.041 (0.027)	-0.041 (0.027)	-0.056* (0.027)	-0.054* (0.024)	nan
Num.Obs.	7214	7214	7214	7214	7214
BIC	25569.5	25562.2	25612.7	25567.4	25703.1

To evaluate the robustness of our findings, we estimated several alternative model specifications presented in Table A6. The first column reproduces our full model used in the main analysis. Each subsequent column systematically excludes a set of related covariates—slope, population, fuel, and weather—to assess the sensitivity of our estimates to specific predictor domains.

Overall, the direction and significance of most coefficients remain stable across specifications, particularly for GHM and tmmx, indicating strong and consistent effects. Notably, removing weather variables slightly attenuates some associations and increases the BIC, suggesting that weather contributes meaningfully to model fit. Dropping slope or population-related terms had minimal impact on other coefficients, while the removal of fuel variables slightly shifted the estimates of related predictors. These results support the robustness of our core findings, with minor variations in magnitude attributable to shared variance across covariates rather than fundamental instability in the model.

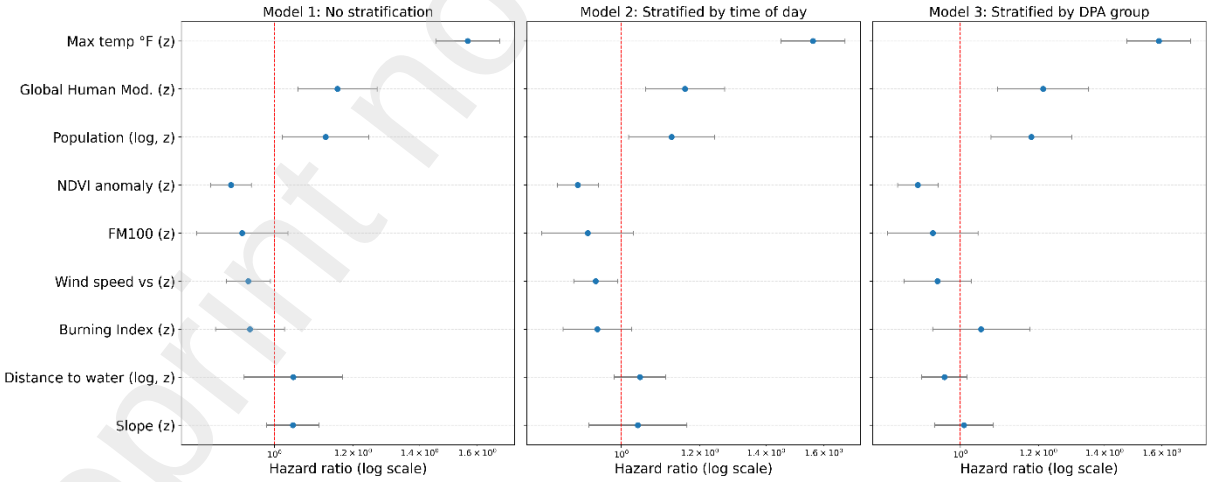

Figure A7. Hazard ratios and 95% confidence intervals from three Cox proportional hazards models evaluating factors influencing the timing of initial aircraft dispatch. Each panel corresponds to a different model specification: (left) Model 1 with no stratification, (center) Model 2 stratified by time of day (morning, afternoon, night), and (right) Model 3 stratified by GACC region (ONCC vs OSCC). The red dashed vertical line at HR = 1 denotes the null effect.

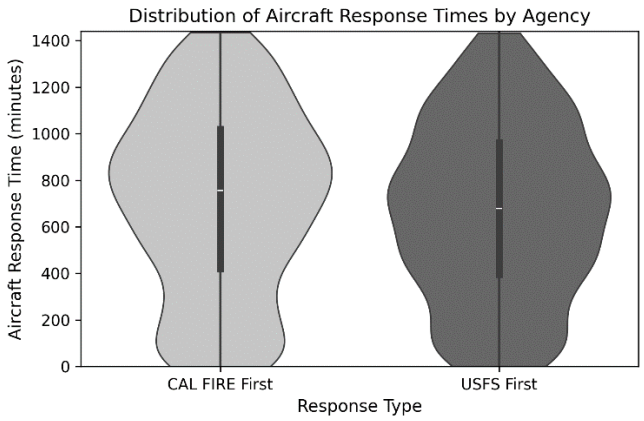

Figure 38. Violin plots comparing aircraft response times for fires first reached by CAL FIRE versus USFS during the 2020 season.

During the preparation of this work, the authors used an AI-based language editing tool to assist with grammar, spelling, and clarity. After using this tool, the authors reviewed and edited the content as needed and take full responsibility for the content of the published article.

Aalen, O.O. and Johansen, S. (1978) 'An empirical transition matrix for non-homogeneous Markov chains based on censored observations', *Scandinavian journal of statistics*, pp. 141–150.

Abatzoglou, J.T. (2013) 'Development of gridded surface meteorological data for ecological applications and modelling', *International journal of climatology*, 33(1), pp. 121–131.

Ali, B.S. (2016) 'System specifications for developing an Automatic Dependent Surveillance-Broadcast (ADS-B) monitoring system', *International Journal of Critical Infrastructure Protection*, 15, pp. 40–46.

Andrews, P.L., Loftsgaarden, D.O. and Bradshaw, L.S. (2003) 'Evaluation of fire danger rating indexes using logistic regression and percentile analysis', *International Journal of Wildland Fire*, 12(2), pp. 213–226.

Bakowski, D.L., Martin, L., Dustin, G. and Mariano, C. (2024) 'Incorporating UAS Traffic Management into Wildland Firefighting Operations: Initial Findings of Subject Matter Expert Interviews', in *2024 AIAA DATC/IEEE 43rd Digital Avionics Systems Conference (DASC)*. IEEE, pp. 1–10.

Bayham, J. and Bryan, C. (2023) 'The Economics of Wildland Firefighting Aviation Procurement and Effectiveness', in *Western Economics Forum*, pp. 43–52.

Bayham, J. and Yoder, J.K. (2020) 'Resource allocation under fire', *Land Economics*, 96(1), pp. 92–110.

Breslow, N. (1974) 'Covariance analysis of censored survival data', *Biometrics*, pp. 89–99.

CAL FIRE (2025) 'Aviation Program'. California Department of Forestry and Fire Protection (CAL FIRE). Available at: https://www.fire.ca.gov/what-we-do/fire-protection/aviation-program.

California Department of Fish and Wildlife (2025) 'California Lakes'. California Department of Fish and Wildlife. Available at: https://gis.data.ca.gov/datasets/CDFW::california-lakes-1.

Congressional Research Service (2023) *Federal Interagency Wildfire Response Framework*. IF12384. Library of Congress. Available at: https://www.congress.gov/crs_external_products/IF/PDF/IF12384/IF12384.3.pdf.

Cox, D.R. (1972) 'Regression models and life-tables', *Journal of the Royal Statistical Society: Series B (Methodological)*, 34(2), pp. 187–202.

Federal Aviation Administration (2020) 'Electronic Code of Federal Regulations: 14 CFR § 91.225 - Automatic Dependent Surveillance-Broadcast (ADS-B) Out equipment and use'. Available at: https://www.ecfr.gov/current/title-14/chapter-I/subchapter-F/part-91/subpart-C/section-91.225 (Accessed: 19 August 2023).

Fillmore, S.D., McCaffrey, S., Bean, R., Evans, A.M., Iniguez, J., Thode, A., Smith, A.M. and Thompson, M.P. (2024) 'Factors influencing wildfire management decisions after the 2009 US federal policy update', *International journal of wildland fire*, 33(1).

Fogarty, L. and Slijepcevic, A. (1998) 'The influence of wind speed on the effectiveness of aerial fire suppression', *Fire Technology Transfer Note* [Preprint], (17).

Grambsch, P.M. and Therneau, T.M. (1994) 'Proportional hazards tests and diagnostics based on weighted residuals', *Biometrika*, 81(3), pp. 515–526.

Jolly, W.M., Freeborn, P.H., Bradshaw, L.S., Wallace, J. and Brittain, S. (2024) 'Modernizing the US National Fire Danger Rating System (version 4): Simplified fuel models and improved live and dead fuel moisture calculations', *Environmental Modelling & Software*, 181, p. 106181.

Keating, E.G., Morral, A.R., Price, C.C., Woods, D., Norton, D.M., Panis, C., Saltzman, E. and Sanchez, R. (2012) *Air attack against wildfires: understanding US Forest Service requirements for large aircraft*. Rand Corporation.

Keeley, J. and Syphard, A. (2021) 'Large California wildfires: 2020 fires in historical context, Fire Ecol., 17, 22'.

Kennedy, C.M., Oakleaf, J.R., Theobald, D.M., Baruch-Mordo, S. and Kiesecker, J. (2019) 'Managing the middle: A shift in conservation priorities based on the global human modification gradient', *Global change biology*, 25(3), pp. 811–826.

Leonardi, M. (2018) ‘ADS-B anomalies and intrusions detection by sensor clocks tracking’, *IEEE Transactions on Aerospace and Electronic Systems*, 55(5), pp. 2370–2381.

Magstadt, S., Wei, Y., Pietruszka, B.M. and Calkin, D.E. (2024) ‘A Deep Learning Approach for Predicting Aerial Suppressant Drops in Wildland Firefighting Using Automatic Dependent Surveillance–Broadcast Data’, *Fire*, 7(11), p. 380.

Martin, L., Arbab, Y., Roberts, L., Mercer, J., Walter, C., McCarty, W. and Sheehe, C. (2022) ‘Developing an Unmanned Aircraft System Pilot Kit (UASP-kit) for Wildland Fire UAS Operators’, in *AIAA AVIATION 2022 Forum*, p. 4003.

McNorton, J.R. and Di Giuseppe, F. (2024) ‘A global fuel characteristic model and dataset for wildfire prediction’, *Biogeosciences*, 21(1), pp. 279–300.

NASA JPL (2020) ‘NASADEM Merged DEM Global 1 arc-second V001 [Data set]’. Available at: https://doi.org/10.5067/MEASUREs/NASADEM/NASADEM_HGT.001.

National Interagency Coordination Center (NICC) (2023) *National Interagency Mobilization Guide*. 2023rd edn. Boise, ID: National Interagency Fire Center. Available at: https://www.nifc.gov/sites/default/files/NICC/3-Logistics/Reference%20Documents/Mob%20Guide/Mobilization_Guide.pdf.

Olive, X., Sun, J., Lafage, A. and Basora, L. (2020) ‘Detecting events in aircraft trajectories: Rule-based and data-driven approaches’, in *Proceedings*. MDPI, p. 8.

Page, W.G. and Butler, B.W. (2018) ‘Fuel and topographic influences on wildland firefighter burnover fatalities in Southern California’, *International journal of wildland fire*, 27(3), pp. 141–154.

Pimlott, K., Laird, J. and Brown Jr, E.G. (2015) ‘Wildfire activity statistics’, *California Department of Forestry and Fire Protection Office of the StateFire Marshal*, pp. 1–45.

Porter, T.W., Crowfoot, W. and Newsom, G. (2020) ‘Wildfire Activity Statistics’, *California Department of Forestry and Fire Protection: Sacramento, CA, USA*, p. 46.

Pourmohamad, Y., Abatzoglou, J.T., Belval, E.J., Fleishman, E., Short, K., Reeves, M.C., Nauslar, N., Higuera, P.E., Henderson, E., Ball, S., and others (2023) ‘Physical, social, and biological attributes for improved understanding and prediction of wildfires: FPA FOD-attributes dataset’, *Earth System Science Data Discussions*, 2023, pp. 1–29.

Reinke, K., Jones, S., Ramsey, S. and Trihantoro, N. (2021) *Utility of Himawari-8 Observations to Explore Aerial Suppression Activities*. Research Report. Melbourne: CSIRO and Bushfire and Natural Hazards CRC.

Rollins, M.G. (2009) ‘LANDFIRE: a nationally consistent vegetation, wildland fire, and fuel assessment’, *International Journal of Wildland Fire*, 18(3), pp. 235–249.

Rothermel, R.C. (1986) *Modeling moisture content of fine dead wildland fuels: input to the BEHAVE fire prediction system*. United States Department of Agriculture, Forest Service, Intermountain … (359).

Safford, H.D., Paulson, A.K., Steel, Z.L., Young, D.J.N. and Wayman, R.B. (2022) 'The 2020 California fire season: A year like no other, a return to the past or a harbinger of the future?', *Global Ecology and Biogeography*, 31(10), pp. 2005–2025. Available at: https://doi.org/10.1111/geb.13498.

Schäfer, M., Strohmeier, M., Lenders, V., Martinovic, I. and Wilhelm, M. (2014) 'Bringing up OpenSky: A large-scale ADS-B sensor network for research', in *IPSN-14 Proceedings of the 13th International Symposium on Information Processing in Sensor Networks*. IEEE, pp. 83–94.

Schafer, M., Strohmeier, M., Smith, M., Fuchs, M., Pinheiro, R., Lenders, V. and Martinovic, I. (2016) 'OpenSky report 2016: Facts and figures on SSR mode S and ADS-B usage', in *2016 IEEE/AIAA 35th Digital Avionics Systems Conference (DASC)*. IEEE, pp. 1–9.

Schoenfeld, D. (1982) 'Partial residuals for the proportional hazards regression model', *Biometrika*, 69(1), pp. 239–241.

Short, K.C. (2022) 'Spatial wildfire occurrence data for the United States, 1992-2020 [FPA_FOD_20221014]'.

Stonesifer, C., Bryan, C., Bayham, J., Calkin, D. and Belval, E. (2022) 'Firefighting aircraft: understanding current practices to shape future response in a changing world', *Environmental Sciences Proceedings*, 17(1), p. 50.

Stonesifer, C.S., Calkin, D.E., Thompson, M.P. and Stockmann, K.D. (2016) 'Fighting fire in the heat of the day: an analysis of operational and environmental conditions of use for large airtankers in United States fire suppression', *International Journal of Wildland Fire*, 25(5), pp. 520–533.

Stonesifer, C.S., Thompson, M.P., Calkin, D. and McHugh, C.W. (2015) 'Characterizing large airtanker use in United States fire management', in *In: Keane, Robert E.; Jolly, Matt; Parsons, Russell; Riley, Karin. Proceedings of the large wildland fires conference; May 19-23, 2014; Missoula, MT. Proc. RMRS-P-73. Fort Collins, CO: US Department of Agriculture, Forest Service, Rocky Mountain Research Station. p. 314-316.*, pp. 314–316.

Strohmeier, M., Olive, X., Lübbe, J., Schäfer, M. and Lenders, V. (2021) 'Crowdsourced air traffic data from the OpenSky Network 2019–2020', *Earth System Science Data*, 13(2), pp. 357–366.

Struminska, A. and Filippone, A. (2024) 'Flight performance analysis of aerial fire fighting', *The Aeronautical Journal*, pp. 1–29.

Sun, J., Vû, H., Ellerbroek, J. and Hoekstra, J.M. (2019) 'pyModeS: Decoding Mode-S Surveillance Data for Open Air Transportation Research', *IEEE Transactions on Intelligent Transportation Systems* [Preprint]. Available at: https://doi.org/10.1109/TITS.2019.2914770.

Taber, M.A., Elenz, L.M. and Langowski, P.G. (2013) 'Decision making for wildfires: A guide for applying a risk management process at the incident level', *Gen. Tech. Rep. RMRS-GTR-298WWW. Fort Collins, CO: US Department of Agriculture, Forest Service, Rocky Mountain Research Station. 59 p.*, 298.

Thompson, M.P. and Calkin, D.E. (2011) ‘Uncertainty and risk in wildland fire management: a review’, *Journal of environmental management*, 92(8), pp. 1895–1909.

Thompson, M.P., Lauer, C.J., Calkin, D.E., Rieck, J.D., Stonesifer, C.S. and Hand, M.S. (2018) ‘Wildfire response performance measurement: current and future directions’, *Fire*, 1(2), p. 21.

U.S. Department of Agriculture, Forest Service (2020) *Aerial Firefighting Use and Effectiveness (AFUE) Report*. Washington, D.C.: U.S. Department of Agriculture. Available at: URL if available.

U.S. Forest Service (2021a) ‘CY2020 U.S. Forest Service Aviation Annual Report’. U.S. Department of Agriculture, Forest Service. Available at: https://www.fs.usda.gov/sites/default/files/2021-06/CY2020_USFSAviationReport_Final_1.pdf.

U.S. Forest Service (2021b) ‘Interagency Aviation Information Bulletin 2021-08’. Available at: https://www.fs.usda.gov/sites/default/files/2022-06/iaib-2021-08.pdf.

U.S. Forest Service (2023) ‘Aviation Strategic Plan 2022-2026’. Available at: https://www.fs.usda.gov/sites/default/files/2023-06/Aviation-Strategic-Plan22-26.pdf.

Varga, M., Polgár, Z.A. and Hedeşiu, H. (2015) ‘ADS-B based real-time air traffic monitoring system’, in *2015 38th International Conference on Telecommunications and Signal Processing (TSP)*. IEEE, pp. 215–219.

Vermote, E. (2019) ‘NOAA climate data record (CDR) of AVHRR normalized difference vegetation index (NDVI), version 5’, *NOAA National Centers for Environmental Information*, 10, p. V5ZG6QH9.

WorldPop and CIESIN (2018) ‘Global high-resolution population density (1\,km) – UN adjusted: United States of America, 2020’. WorldPop, University of Southampton. Available at: https://dx.doi.org/10.5258/SOTON/WP00674.

Title Page

An Assessment of Aerial Firefighting Response Times Between Agencies During the 2020 Fire Season in California

Authors:

Shayne Magstadt
Department of Forest and Rangeland Stewardship, Colorado State University
1472 Campus Delivery, Fort Collins, CO 80523, USA

Erin J. Belval
Human Dimensions Science Program, Rocky Mountain Research Station
USDA Forest Service
Fort Collins, CO 80526, United States of America

Bradley M. Pietruszka
Human Dimensions Program, Rocky Mountain Research Station
USDA Forest Service
240 W Prospect Road, Fort Collins, CO 80526, USA

Yu Wei
Department of Forest and Rangeland Stewardship, Colorado State University
1472 Campus Delivery, Fort Collins, CO 80523, USA

Christopher O'Connor
United States Department of Agriculture, Forest Service
Rocky Mountain Research Station
800 East Beckwith Avenue, Missoula, MT 59801, USA

Corresponding Author:
Shayne Magstadt
Email: *Shayne.Magstadt@colostate.edu*

Funding Statement:

Funding was provided through a Challenge Cost Share Agreement between Colorado State University and the U.S. Forest Service, Rocky Mountain Research Station (Agreement No. 22-CS-11221636-189).

Acknowledgements:
The authors thank the OpenSky Network for providing open access to ADS-B data and acknowledge the U.S. Forest Service for making operational and contextual information available.